4. THE AMPLITUDE PROBABILITY DISTRIBUTION

As noted in the introduction, atmospheric noise (and most forms of man-made noise) is a random process. This means that the noise can be described only in probabilistic terms. The basic distribution of any random process is its first order probability density function (pdf) or distribution function, and a random process is said to be completely described by its hierarchy of density functions (first order, second order, and so on, ad infinitum).

The received atmospheric noise process under consideration here is a bandpass process in that it is describable by an envelope process and a phase process. That is, the received noise process is given by

$$N(t) = E(t) \cos [\omega_c t + \phi(t)], \tag{26}$$

where $E(t)$ is the envelope process and $\phi(t)$ is the phase process and ω_c is the bandpass filter center frequency. Since the phase process is known (phase uniformly distributed), the required pdf of the instantaneous amplitude can be obtained from the envelope amplitude pdf. Usually, also, the envelope pdf can be used directly in system performance analyses. The atmospheric noise envelope statistic is usually given as (and measured as) a cumulative exceedance distribution, termed the "amplitude probability distribution" or APD. The APD was described earlier (11) and is given by the probability of the envelope level E (26) being above the level E_i;

$$D(E) = \text{Prob}[E \geq E_i] = 1 - P(E) \tag{27}$$

where $P(E)$ is the cumulative distribution function of the envelope. The pdf of E is given by the derivative of $P(E)$.

Various statistical moments of the received noise envelope were defined earlier. Of concern here are the parameters V_d (15) and L_d (16). Crichlow et al. (1960a) developed a "model" or method of obtaining the APD from these two measured statistical moments. A "most likely" subset of this model became the "CCIR Report 322" model (1964). CCIR Report 322 also gives estimates of V_d (for a 200-Hz bandwidth). One of the purposes here is to review this model and present a numerical representation, including bandwidth relationships, since the received APD is a function of the receiver bandwidth. There have been many models for atmospheric (and other) noise developed over the years, with the CCIR ad hoc model for the APD being one of the many models. A historical summary of the various main models and their interrelationships has been given by Spaulding (1977, 1982) and by Shaver et al. (1972).

4.1 The CCIR 322 APD Model

Using all the measured distributions (APD) of the received atmospheric radio noise envelope available at the time (a small number compared to what is available today), Crichlow et al. (1960a) developed an APD model, where the APD is represented by two straight lines connected by the arc of a circle on a particular coordinate system. The coordinate system used is given by the ordinate being the envelope voltage level (in dB) and the abscissa being the percentage of time the ordinate is exceeded. The coordinates are such that the Rayleigh distribution (envelope of Gaussian noise) plots as a straight line of slope -1/2. These coordinates are log of voltage versus $-1/2 \log_{10}$ (-ln of probability). Figure 82 shows these coordinates, an APD composed of the two straight lines and the circular arc, and the parameters that were used to define this idealized APD. The low envelope level-high probability straight line is a Rayleigh distribution, since the noise process must approach Rayleigh at the lower voltage levels. The parameters used (Figure 82) are defined as follows:

A = dB difference between Rayleigh at 0.5 probability and the E_{rms} level.

B = dB difference between the point of intersection of the Rayleigh and high-voltage, low probability line and the tangent to the circular arc (the tangent being drawn perpendicular to the bisector of the angle formed by the Rayleigh and high-voltage, low probability line).

C = dB difference between the high-voltage, low probability line and Rayleigh line at 0.01 probability coordinate.

X = absolute value of slope of high-voltage, low probability line relative to Rayleigh, that is $X = -2\ m_2$, where m_2 is the slope of the high-voltage, low probability line.

Next, it was shown that B could be given, approximately, as

$$B = 1.5(X - 1). \tag{28}$$

Figure 83 shows the correlation of B with X for the measured distributions available at the time. A number of APD's were drawn for a range of values of X, C, and A (the remaining unknowns). These distributions were numerically integrated (essentially by hand) and V_d and L_d determined for each APD. From these integrations, X and C were obtained as functions of V_d and L_d, and A was obtained as a function of X and C.

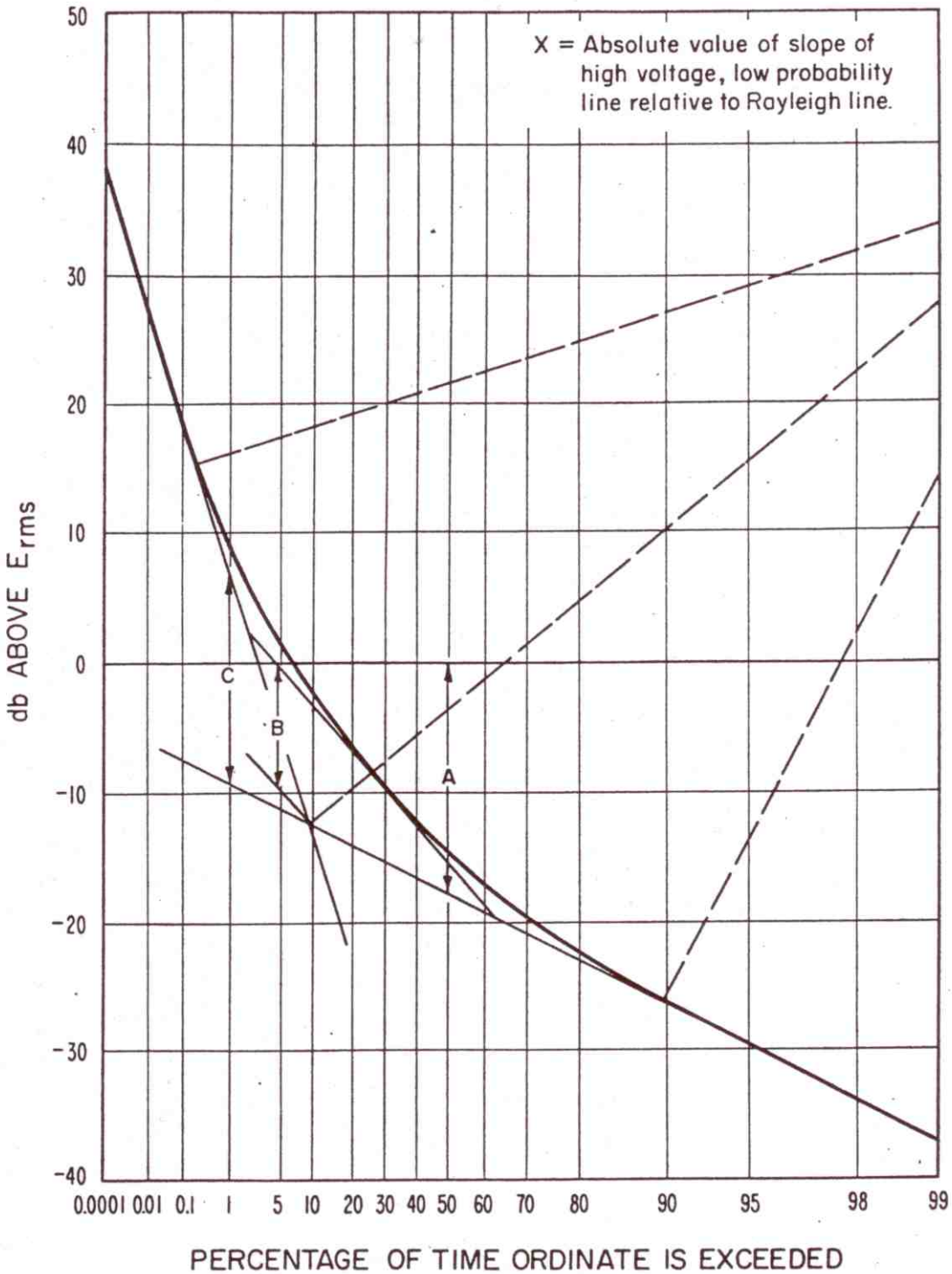

Figure 32. Definition of parameters for the amplitude probability distribution of atmospheric radio noise.

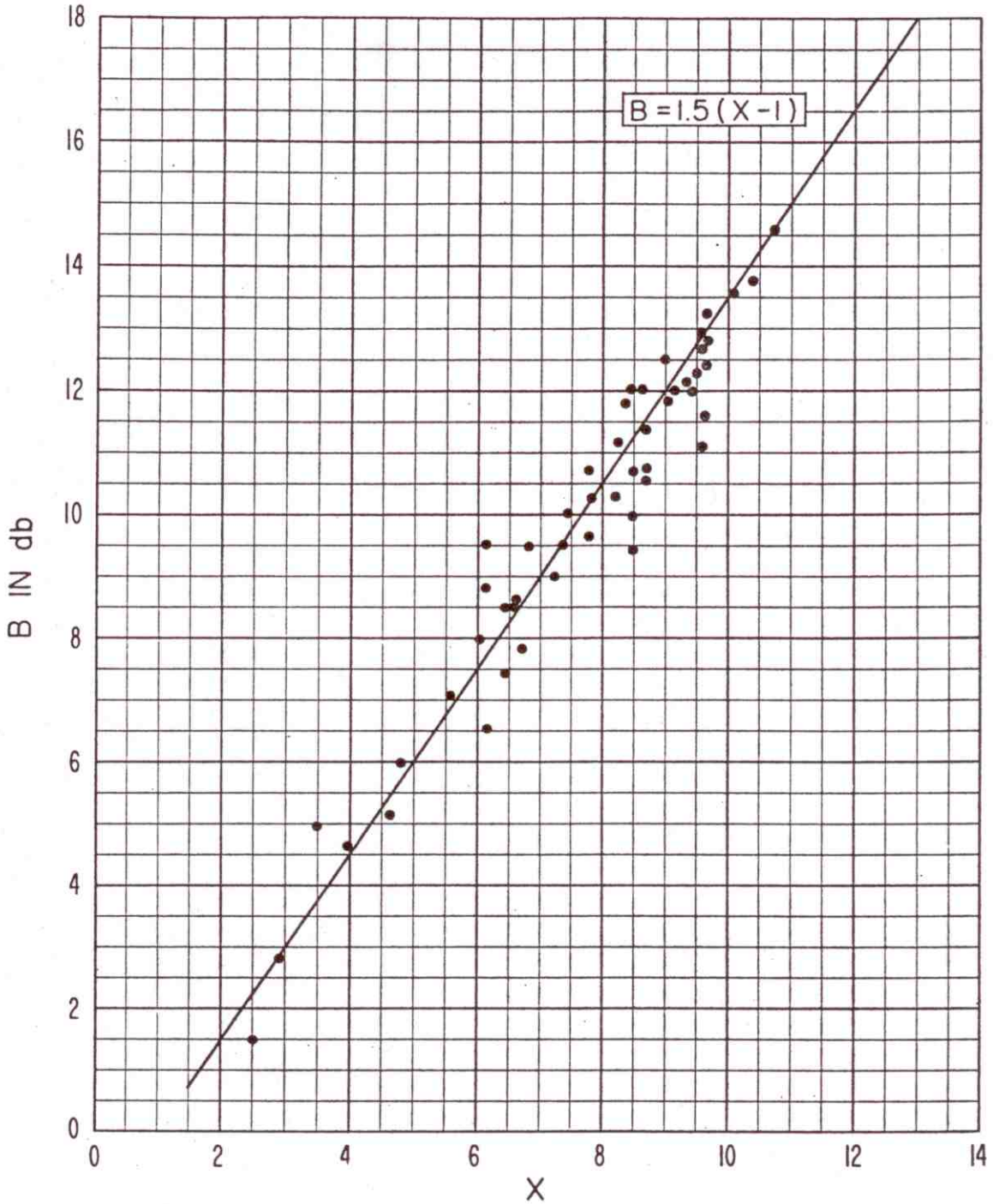

Figure 83. Experimental correlation of B and X.

Figures 84, 85, and 86 show these functional relationships. Use of these results allowed construction of an APD for any measured V_d-L_d combination, and these constructions did represent the measured APD's rather well. Crichlow et al. (1960b) presented sets of APD's, a set for each V_d along with the allowed range of L_d's for that particular V_d.

The APD is a function of receiver bandwidth, and when developing a method to convert the APD appropriate in one bandwidth to that which would be observed in another bandwidth, Spaulding et al. (1962) noted that V_d and L_d were highly correlated. Using approximately 95 measured distributions, the majority measured in a 200 Hz bandwidth and various frequencies between 13 kHz and 20 MHz, it was shown that the linear correlation of L_d with V_d is given by

$$L_d = 1.697\ V_d + 0.7265 \quad . \tag{29}$$

A few of the above distributions were measured in other than a 200 Hz bandwidth. These bandwidths were 0.64 Hz, 6 Hz, 10 Hz, 170 Hz, 950 Hz, and 1170 Hz. APD's measured since in wider bandwidths appear to be still representable by the above model. For example, Figure 87 shows an APD of atmospheric noise measured at 4.75 MHz in a 50 kHz bandwidth along with the "CCIR APD" for a V_d of 8.6 dB. The relationship (29) was used to develop the "standard" set of APD's given in CCIR Report 322. The linear correlation (29) gives results for small V_d that are not mathematically valid. For example, for a V_d of 2 dB, say, the resulting value of 4.12 dB for L_d is not mathematically possible. Therefore, the relationship (29) has to be relaxed slightly in order to obtain APD's for the smaller value of V_d($\leq$5 dB), and this modification is arbitrary. The dashed curves on Figures 84 and 85 show the relationship (29) and, therefore, the particular APD's that compose the CCIR 322 model. This set of APD's is given on Figure 88.

A mathematical representation of the APD using the above model was developed some time ago for computer use. This development was never documented, but was used by various authors in system performance studies. See, for example, Conda (1965), Halton and Spaulding (1966), and Spaulding (1966). The input parameters to these computer algorithms are X, C, and A, obtained graphically from figures such as 84, 85, and 86.

In the next section, we present the geometry of the APD model and a computer algorithm for the "standard" set of APD's where the input is V_d directly. This is based on earlier results by Akima (1972). The "standard" set of APD's obtained from this algorithm will be seen to be slightly different from the earlier CCIR 322

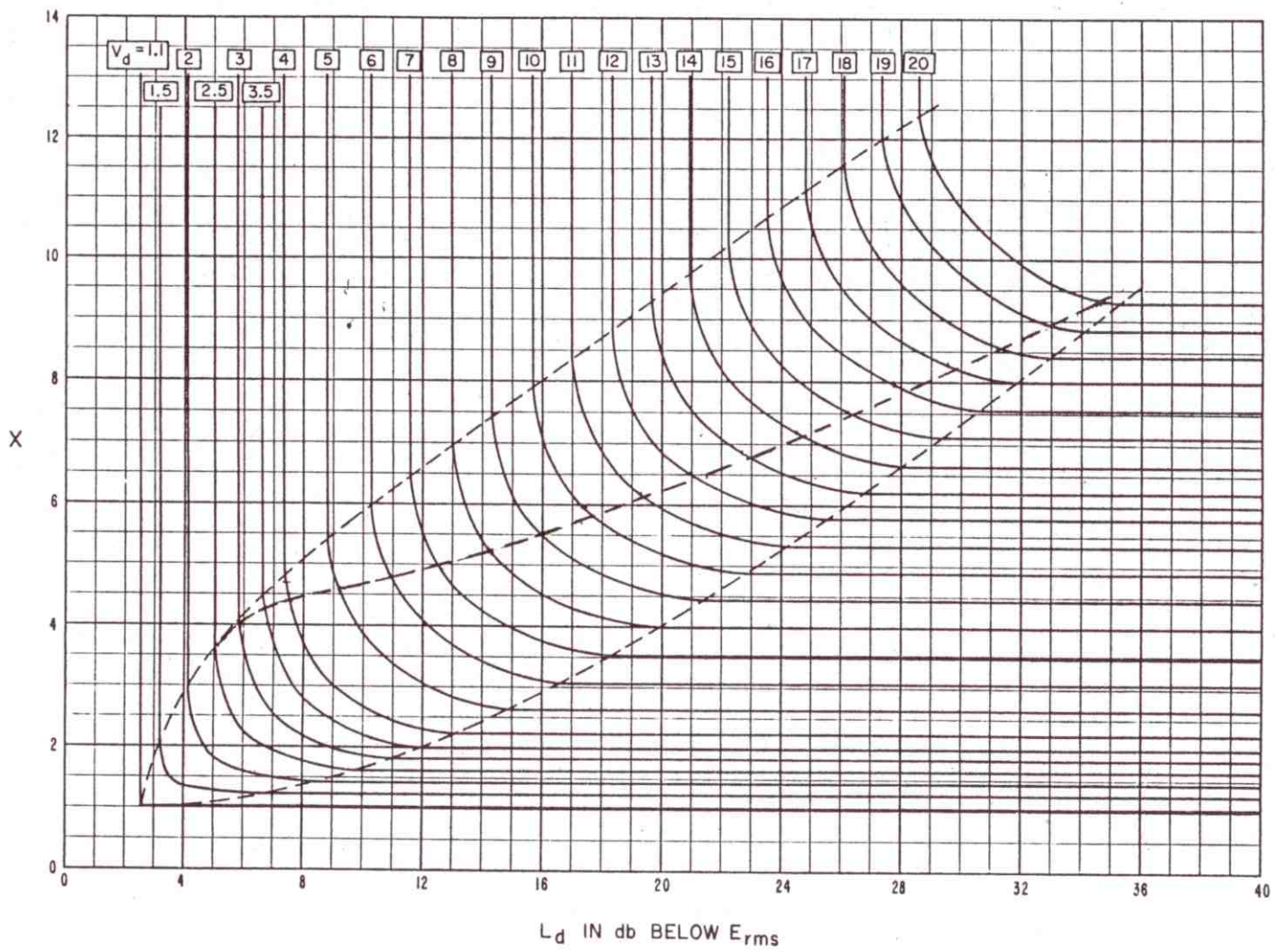

Figure 84. X versus L_d and V_d.

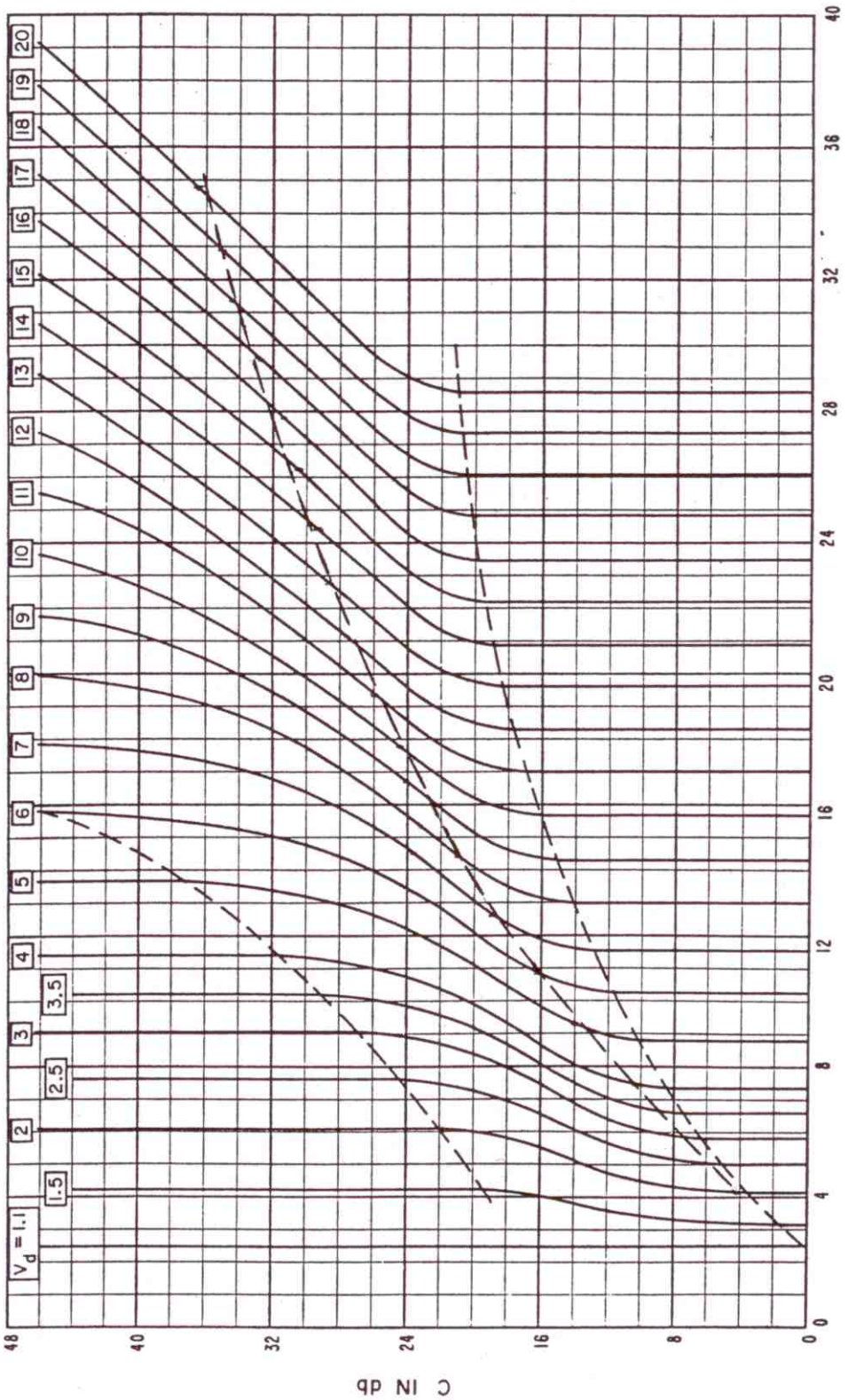

Figure 85. C versus L_d and V_d.

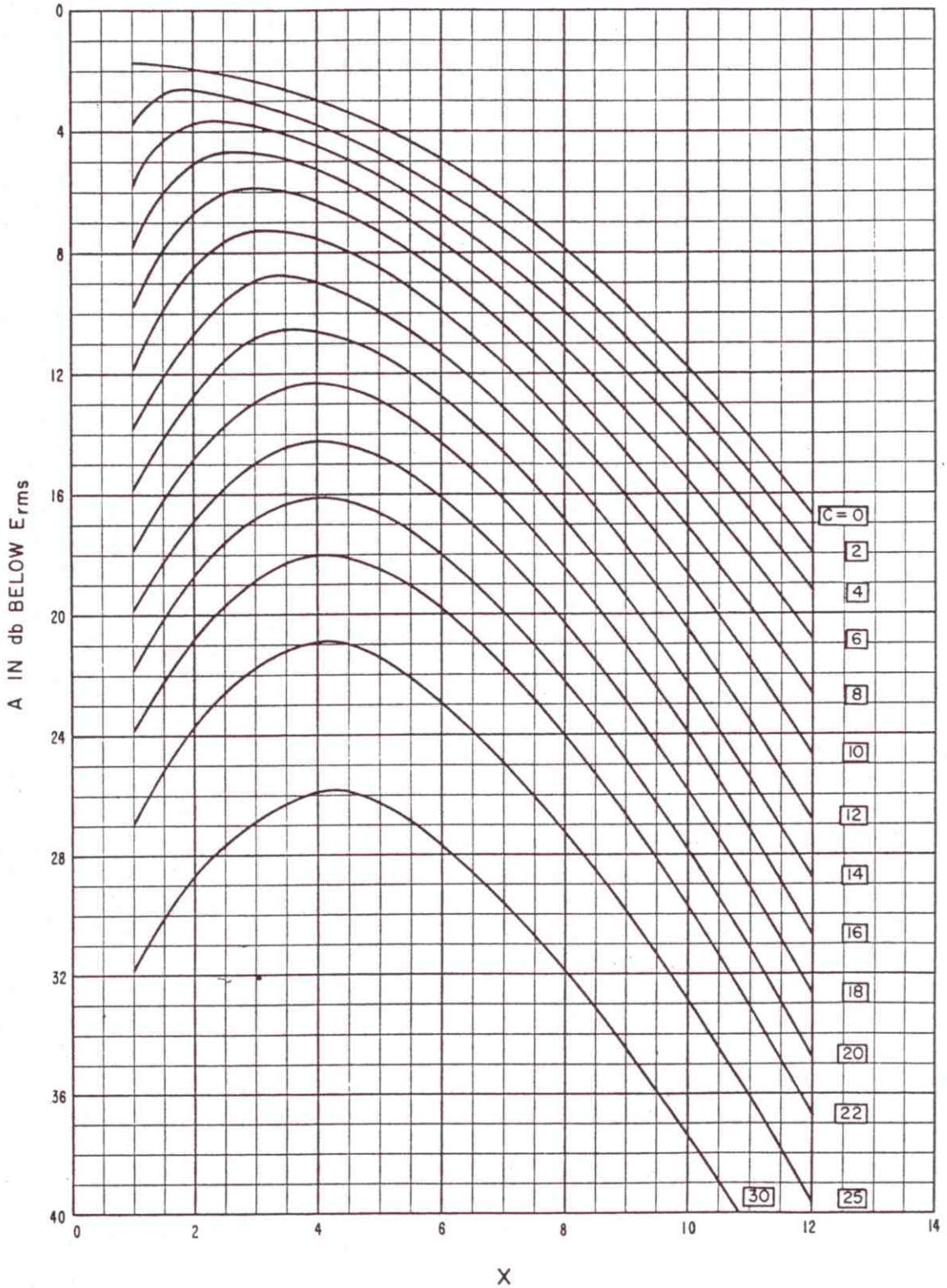

Figure 86. A versus X and C.

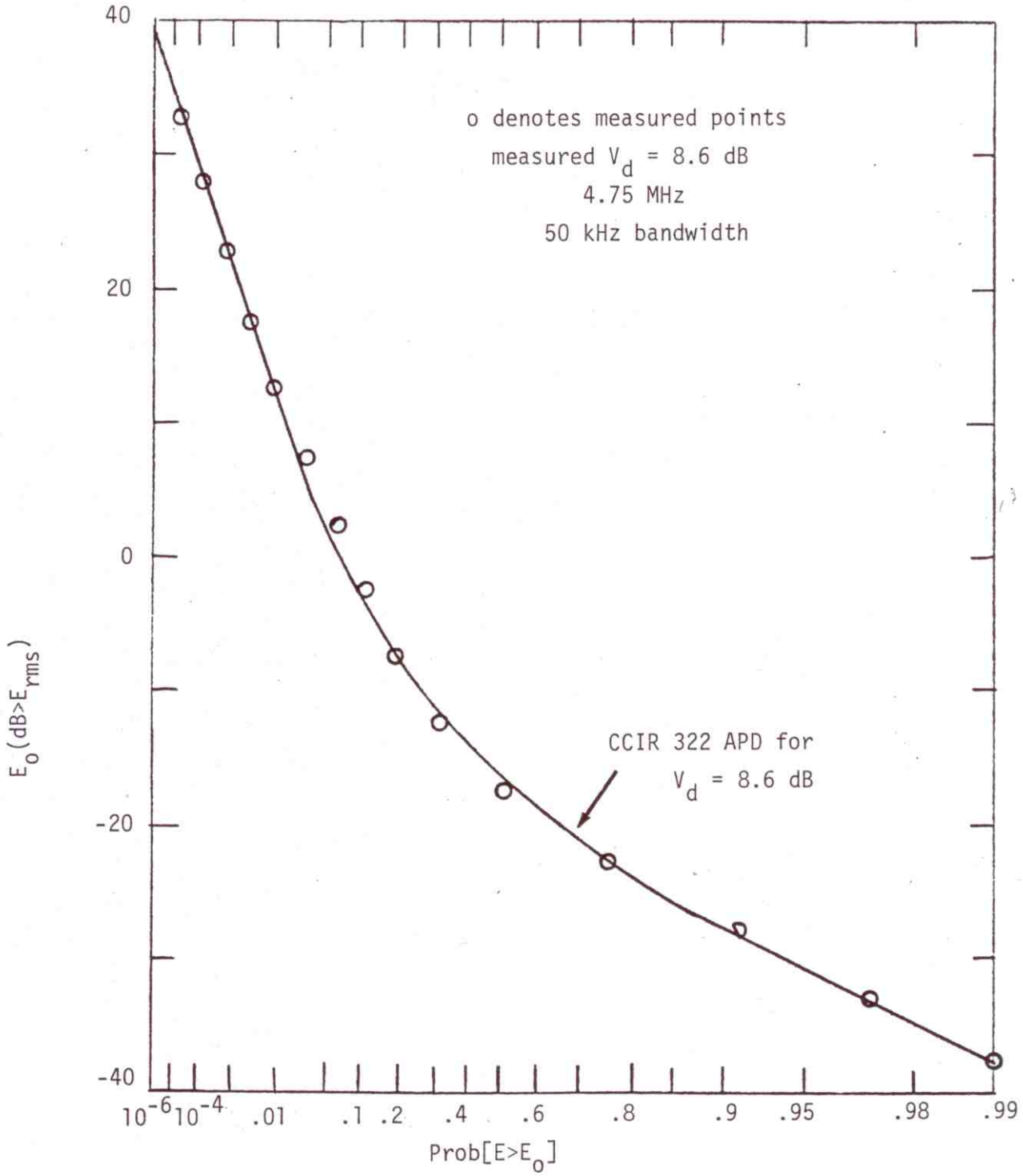

Figure 87. An APD of atmospheric radio noise measured at 4.75 MHz in a 50 kHz bandwidth (15 seconds of data) compared with the CCIR Report 322 APD for a V_d of 8.6 dB.

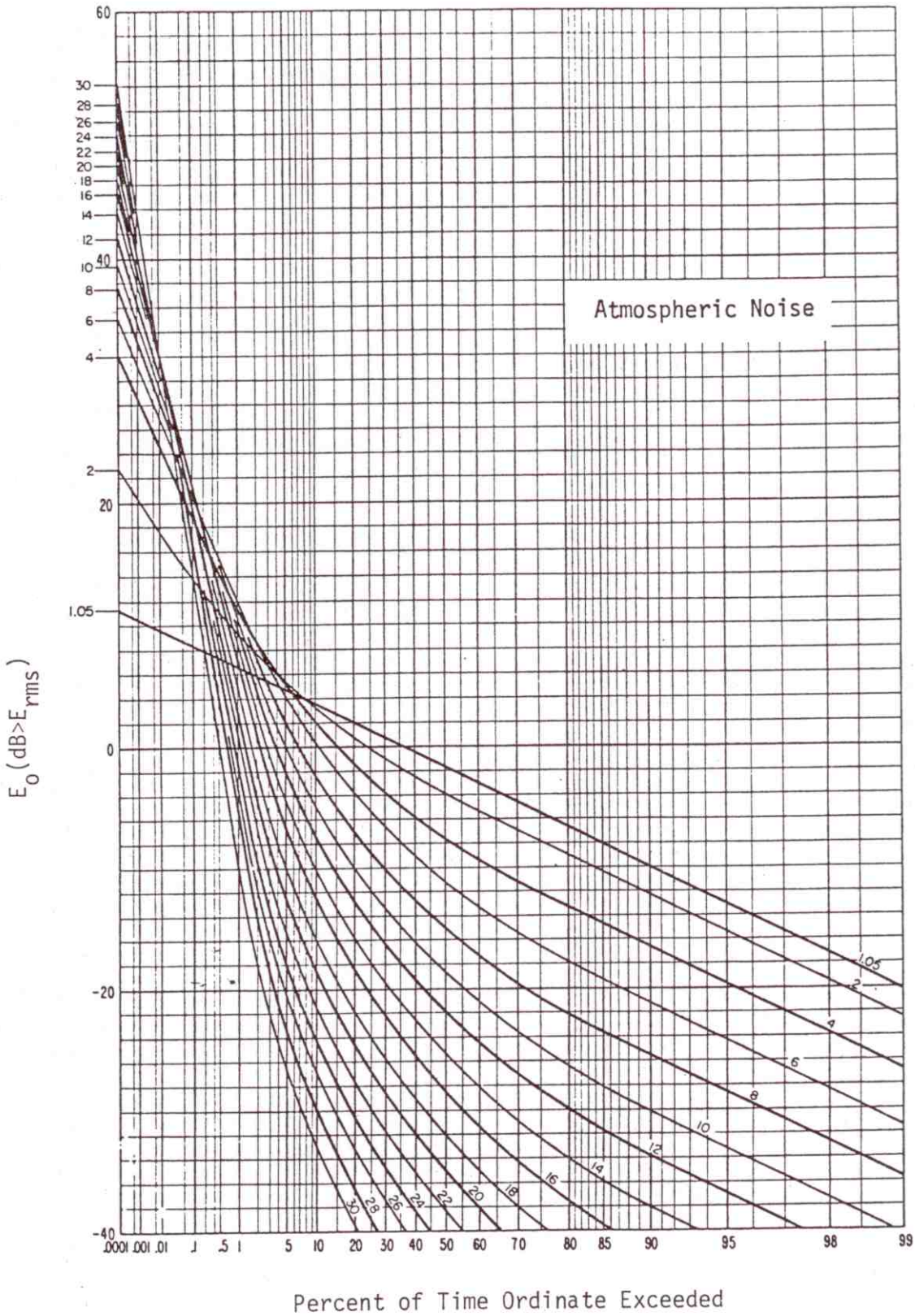

Figure 88. CCIR Report 322 set of amplitude probability distributions of atmospheric radio noise for various V_d values.

standard set (Figure 88) for the smaller values of V_d. This is due to much more precise numerical integration of the APD's and determination of the relationship between the parameters defining the APD's and the corresponding V_d's and L_d's. Also, a more physically meaningful modification of the linear regression (29) was used (See Akima, 1972).

In order to use the computer algorithm or the corresponding set of graphical APD's (Figure 88), the appropriate V_d for the required bandwidth must be determined. CCIR Report 322 gives estimates of V_d for each season and time block for frequencies between 10 kHz and 20 MHz. These values of V_d are for a 200 Hz bandwidth. The bandwidth conversion of V_d will be treated in a later section. The CCIR 322 V_d estimates were obtained by fitting the function

$$V_d(x) = c_0 + c_1 x + c_2 x^2 + c_3 x^3 + c_4 x^4 \quad , \tag{30}$$

where $x = \log_{10}(f_{MHz})$,

and f_{MHz} is the frequency in MHz.

Table 41 gives the sets of c coefficients for each season and time block to be used with (30) to obtain the CCIR Report 322 V_d estimates. It is interesting to note that these coefficients have not been presented previously.

The observed variation of V_d, σ_{V_d}, is also an important statistic for system performance analysis. Table 42 gives sets of d coefficients for each season and time-block for σ_{V_d}, using the relationship (30). That is

$$\sigma_{V_d}(x) = d_0 + d_1 x + d_2 x^2 + d_3 x^3 + d_4 x^4 \quad . \tag{31}$$

CCIR Report does not give σ_{V_d}, but handles the variation of the APD differently. Using (31) is much more appropriate, however, especially for numerical work.

The network of recording stations that made the measurements that produced CCIR Report 322 measured the parameter L_d as well as V_d. Table 41 and 42 give the coefficients for the season time-block estimates of V_d and σ_{V_d}. A similar set of estimates for L_d and σ_{L_d} is now also available, based on all the previous measurements. Tables 43 and 44 give the coefficients [corresponding to (30) and (31) above] for L_d and σ_{L_d} for each season-time block. That is

Table 41. Coefficients for the CCIR Report 322 V_d Estimates, S = Season (1 = Winter, etc.) and TB = Time block (1 = 0000-0400 Hours, etc.).

S	TB	c_4	c_3	c_2	c_1	c_0
1	1	-4.15586022E-01	-7.50869801E-01	-6.26841762E-02	-1.61673242E+00	6.78459487E+00
1	2	-8.19124731E-01	-9.09585597E-01	1.24573700E+00	-1.80429429E+00	6.43835525E+00
1	3	-1.42224362E+00	-1.18235587E+00	4.15636528E+00	-1.31952622E+00	4.14994576E+00
1	4	-1.43530592E+00	-1.40729681E+00	4.30851317E+00	-6.13432992E-01	3.97698107E+00
1	5	-9.13614531E-01	-1.02085307E+00	2.05263792E+00	-1.20481693E+00	5.76797550E+00
1	6	-5.00808267E-01	-6.40179441E-01	6.00336702E-01	-1.72489385E+00	6.28328251E+00
2	1	-4.10306784E-01	-5.59607899E-01	8.41784321E-03	-1.82745777E+00	7.01077413E+00
2	2	-9.17965965E-01	-8.57576457E-01	1.65778832E+00	-1.74210229E+00	6.31934305E+00
2	3	-1.25456604E+00	-8.33540325E-01	3.35449427E+00	-2.02941542E+00	5.61265781E+00
2	4	-8.64337002E-01	-3.66203002E-01	2.43257460E+00	-2.43853742E+00	6.02758044E+00
2	5	-5.30065572E-01	-2.18096252E-01	1.28866179E+00	-2.14385922E+00	6.00629093E+00
2	6	-4.17496112E-01	-3.94890710E-01	5.65160173E-01	-1.81148452E+00	6.28661034E+00
3	1	-1.68487571E-01	-4.83367793E-01	-4.73701322E-01	-1.72666100E+00	7.16722078E+00
3	2	-9.15337559E-01	-8.83815317E-01	1.66817783E+00	-2.18486442E+00	7.16769077E+00
3	3	-1.13551135E+00	-7.83533518E-01	2.75493715E+00	-2.32068743E+00	6.72491255E+00
3	4	-1.98417811E-01	3.01961060E-02	-2.64713855E-01	-2.60622295E+00	8.18005102E+00
3	5	1.02759914E-02	2.09493861E-01	-6.30085802E-01	-2.55700412E+00	7.18374974E+00
3	6	-1.80634032E-01	-2.06153419E-01	2.48345237E-01	-1.81286248E+00	5.73012908E+00
4	1	-2.39386843E-01	-4.96995642E-01	-5.10797542E-01	-2.14213999E+00	7.56139657E+00
4	2	-8.38309477E-01	-7.03483344E-01	1.51059375E+00	-2.36513950E+00	6.94308817E+00
4	3	-1.70706706E+00	-1.17987406E+00	4.82706183E+00	-1.76485628E+00	5.06494256E+00
4	4	-1.41821434E+00	-1.11527452E+00	3.86485170E+00	-1.40866619E+00	5.21901993E+00
4	5	-7.11876529E-01	-6.18844507E-01	1.52472219E+00	-1.78588700E+00	6.06417207E+00
4	6	-3.99560349E-01	-4.70927657E-01	4.68497339E-01	-1.92315743E+00	6.52222929E+00

Table 42. Coefficients for σ_{V_d} Estimates, S = Season (1 = Winter, etc.) and TB = Time-block (1 = 0000-0400 Hours, etc.)

S	TB	d_4	d_3	d_2	d_1	d_0
1	1	5.74559281E-01	4.62707699E-01	-1.72173781E+00	-9.95140894E-01	2.20240447E+00
1	2	4.35458757E-01	4.25522378E-01	-1.60117703E+00	-1.08102724E+00	2.58152223E+00
1	3	-6.49233466E-03	4.74253633E-02	-4.03212846E-01	-6.23938149E-01	2.24785228E+00
1	4	4.81514268E-02	3.88000518E-02	-4.79816376E-01	-7.53047623E-01	2.36761696E+00
1	5	2.20951179E-01	1.04067232E-01	-1.00765279E+00	-7.66812705E-01	2.49052997E+00
1	6	3.06314630E-01	1.51288358E-01	-1.05397392E+00	-5.54183344E-01	1.99341144E+00
2	1	3.86616314E-01	8.01623166E-01	-8.87032696E-01	-1.52905085E+00	1.92759641E+00
2	2	4.40050440E-01	7.18383335E-01	-1.35584006E+00	-1.64482072E+00	2.45213428E+00
2	3	3.67170246E-02	-5.61537089E-02	-1.01505114E+00	-3.83501537E-01	3.09611594E+00
2	4	1.65289800E-01	1.70060547E-02	-1.15989586E+00	-3.09043606E-01	2.85528452E+00
2	5	3.07936037E-01	3.85654734E-01	-1.00679367E+00	-1.02253224E+00	1.98359891E+00
2	6	1.31439752E-01	4.02605087E-01	-4.03779860E-01	-9.92782318E-01	1.70204048E+00
3	1	3.58940314E-01	4.95409368E-01	-8.27121405E-01	-7.63286332E-01	1.55427990E+00
3	2	2.09965713E-01	3.24844698E-01	-8.07822126E-01	-8.80559875E-01	2.08557260E+00
3	3	-9.08564453E-02	-1.75290010E-01	-4.90665403E-01	-1.91890309E-01	2.80704666E+00
3	4	-2.94892431E-04	-2.05446289E-01	-7.68224281E-01	1.17367277E-01	2.75988679E+00
3	5	1.91096116E-01	1.87522643E-01	-9.11250293E-01	-5.71111677E-01	1.98460093E+00
3	6	2.47570773E-01	3.91438655E-01	-6.43926655E-01	-7.67813443E-01	1.49625461E+00
4	1	5.01750036E-01	5.77129399E-01	-1.35720266E+00	-1.04622956E+00	1.99818623E+00
4	2	3.55927079E-01	4.23490372E-01	-1.29001962E+00	-9.61774515E-01	2.30245072E+00
4	3	-5.57814073E-02	-1.21842205E-01	-5.62937765E-01	-3.16487314E-01	2.94384763E+00
4	4	1.07676095E-01	-1.21212315E-01	-9.15292141E-01	-2.77208541E-01	2.97756952E+00
4	5	1.40565912E-01	6.61535051E-02	-6.51440190E-01	-4.10729136E-01	1.86781589E+00
4	6	1.14401727E-01	2.07595064E-01	-3.50865144E-01	-5.22015309E-01	1.52884872E+00

Table 43. Coefficients for L_d Estimates, S = Season (1 = Winter, etc.) and TB = Time block (1 = 0000-0400 Hours, etc.)

S	TB	e_4	e_3	e_2	e_1	e_0
1	1	-4.01080390E-01	-8.06871222E-01	-9.16065607E-01	-3.12341181E+00	1.17796511E+01
1	2	-1.14612417E+00	-1.16044131E+00	1.48801759E+00	-3.11963345E+00	1.08095069E+01
1	3	-2.01268851E+00	-1.58446010E+00	5.76959544E+00	-2.19798985E+00	7.15846402E+00
1	4	-2.01284126E+00	-1.69581923E+00	6.20222659E+00	-1.68630451E+00	6.54887850E+00
1	5	-1.22376561E+00	-1.14145192E+00	2.70535893E+00	-2.57991235E+00	9.57765195E+00
1	6	-4.77566043E-01	-6.80647279E-01	-1.38313271E-01	-3.08912539E+00	1.11620472E+01
2	1	-7.56387723E-01	-9.41795283E-01	1.48878601E-02	-3.01658687E+00	1.19305855E+01
2	2	-1.47380509E+00	-1.13857531E+00	2.70265503E+00	-3.39495783E+00	1.06030690E+01
2	3	-1.64465533E+00	-5.20826651E-01	4.66848576E+00	-4.41871597E+00	9.24596259E+00
2	4	-1.07577532E+00	-6.58190899E-02	3.10458703E+00	-4.52877044E+00	1.00850456E+01
2	5	-6.94420166E-01	-1.16143553E-01	1.54082549E+00	-3.84614111E+00	1.03725134E+01
2	6	-5.44782695E-01	-3.70339547E-01	4.18740539E-01	-3.36683216E+00	1.08592467E+01
3	1	-5.72573485E-02	-6.31460722E-01	-1.67851932E+00	-3.02538520E+00	1.27623885E+01
3	2	-1.21972222E+00	-9.01790378E-01	1.92007436E+00	-4.29975019E+00	1.22139152E+01
3	3	-1.46183941E+00	-6.21479919E-01	3.46372974E+00	-4.72257846E+00	1.12195165E+01
3	4	8.89864683E-02	4.55733588E-01	-1.51999568E+00	-4.74217115E+00	1.37346270E+01
3	5	2.07351893E-01	5.81000648E-01	-1.57227661E+00	-4.50545603E+00	1.23294894E+01
3	6	-1.89484675E-01	-2.32209905E-01	-1.63480903E-01	-3.20050499E+00	1.03548994E+01
4	1	-5.66360041E-02	-4.83281183E-01	-1.97564001E+00	-3.79144519E+00	1.32416806E+01
4	2	-1.12491420E+00	-9.11485568E-01	1.55307102E+00	-3.95085955E+00	1.18725334E+01
4	3	-2.48390336E+00	-1.51620101E+00	6.93839891E+00	-3.15527018E+00	8.45645981E+00
4	4	-1.75758814E+00	-1.19889517E+00	4.88840291E+00	-2.78488101E+00	8.95452079E+00
4	5	-9.24933064E-01	-6.82560000E-01	1.78149730E+00	-3.32249985E+00	1.05203855E+01
4	6	-5.81223504E-01	-5.66027834E-01	3.01275165E-01	-3.53727004E+00	1.13939994E+01

Table 44. Coefficients for σ_{L_d} Estimates, S = Season (1 = Winter, etc.), TB = Time block (1 = 0000-0400 Hours, etc.)

S	TB	f_4	f_3	f_2	f_1	f_0
1	1	9.01312767E-01	7.88067963E-01	-3.00905494E+00	-1.70696299E+00	3.82658841E+00
1	2	8.40212504E-01	8.47490696E-01	-2.98248275E+00	-2.02966382E+00	4.31515747E+00
1	3	-1.15010729E-01	1.14301151E-01	-4.59078531E-01	-1.16383964E+00	3.74010391E+00
1	4	2.38301427E-02	3.19603082E-01	-6.61835101E-01	-1.54605599E+00	3.52091972E+00
1	5	4.18614469E-01	4.50300762E-01	-1.60948778E+00	-1.64255799E+00	3.59113521E+00
1	6	3.48991796E-01	1.98604395E-01	-1.44513230E+00	-9.52923306E-01	3.31937922E+00
2	1	7.48772662E-01	1.35688170E+00	-1.62281902E+00	-2.23630853E+00	2.91318837E+00
2	2	7.71793817E-01	1.18185259E+00	-2.68206137E+00	-2.55304851E+00	4.33849834E+00
2	3	3.32902164E-01	4.53383515E-01	-2.35643875E+00	-1.62755279E+00	5.31224117E+00
2	4	8.49533890E-01	7.58362650E-01	-3.23297819E+00	-1.54336524E+00	5.06695298E+00
2	5	7.49445008E-01	6.62196232E-01	-2.57325195E+00	-1.66050741E+00	3.66111294E+00
2	6	2.04405264E-01	5.28586058E-01	-6.24392010E-01	-1.42954452E+00	2.47515282E+00
3	1	6.88900456E-01	8.03747629E-01	-1.81006419E+00	-1.11791608E+00	2.52498491E+00
3	2	6.16625068E-01	8.19429853E-01	-2.30453767E+00	-1.83898053E+00	3.97380417E+00
3	3	-9.78848747E-02	-2.34615748E-01	-1.12402853E+00	-5.03506352E-01	4.74347300E+00
3	4	3.66977790E-01	-1.42718306E-01	-2.41897240E+00	-2.04556660E-02	4.89462488E+00
3	5	5.48989406E-01	3.22359358E-01	-2.21794175E+00	-6.69402823E-01	3.27316437E+00
3	6	1.56926584E-01	2.18540144E-01	-4.23639121E-01	-4.33381686E-01	1.67025525E+00
4	1	8.22378639E-01	6.85277683E-01	-2.56770690E+00	-1.25328720E+00	3.33183215E+00
4	2	7.37138510E-01	7.90719147E-01	-2.60914502E+00	-1.77202522E+00	4.01696572E+00
4	3	3.29307237E-02	2.61046502E-01	-1.31346784E+00	-1.41271059E+00	4.99214530E+00
4	4	1.36887095E-01	-8.21977668E-02	-1.74000982E+00	-7.00101431E-01	4.87512720E+00
4	5	3.24876972E-01	1.05665674E-01	-1.51298491E+00	-6.94697920E-01	3.21008663E+00
4	6	3.01877516E-01	3.38148064E-01	-1.03299281E+00	-8.80198176E-01	2.63363314E+00

$$L_d(x) = e_0 + e_1 x + e_2 x^2 + e_3 x^3 + e_4 x^4 \quad , \tag{32}$$

and

$$\sigma_{L_d}(x) = f_0 + f_1 x + f_2 x^2 + f_3 x^3 + f_4 x^4 \quad , \tag{33}$$

and, as before

$$x = \log_{10}(f_{MHz}).$$

Figure 89 shows the relationship between the V_d's from (30) and L_d's from (32) using each of the 24 season-time blocks and the 11 measurement frequencies, .013, .051, .120, .160, .246, .495, .545, 2.5, 5, 10, and 20 MHz. These estimates for V_d and L_d are for average values, averaged over the entire Earth's surface and over each season-time block. Note that these average V_d's and L_d's are highly correlated (Figure 89), but that this correlation is somewhat different from that given in (29), which was obtained from a set of actual measured distributions. The relation (29) is also shown on Figure 89 for comparison.

A monograph by V. F. Osinin (1982) presents the results of experimental studies of natural radio noise on frequencies from VLF to HF within auroral, subauroral, and middle-latitude areas of the USSR. Osinin (1982) shows L_d versus V_d relationships obtained from APD measurements for four locations, three in the far eastern USSR and one in Japan. The three USSR locations are M. Schmidt, Magadan, and Khaborovsk. The Soviet measurements are in the frequency range 12 to 10,000 kHz and the measurements from Japan are at 50 kHz with a 1 kHz bandwidth. The bandwidth used for the Soviet measurements is not specified. In all four cases the results are similar to Figure 89 in that V_d and L_d are highly linearly correlated with the individual V_d-L_d points clustering slightly below the $L_d = 1.697V_d + 0.7265$ line (which Osinin also displays).

The APD for man-made noise can also be modeled by the Crichlow et al. (1960a) model. See, for example, Disney and Spaulding (1970), Spaulding et al. (1971), Spaulding and Disney (1974), Spaulding (1976), and Hagn (1982). Figure 90 shows the correlation of L_d with V_d for man-made noise, using 637 measured V_d and corresponding L_d median values for numerous locations throughout the United States and for various frequencies covering the range 250 kHz to 250 MHz and in a 4-kHz bandwidth. Note that the relationship is somewhat different from that for atmospheric radio noise (29). The computer algorithm for the APD presented in the next section has